Separation and Purification Technology 324 (2023) 124496

Contents lists available at ScienceDirect

Separation and Purification Technology

journal homepage: www.elsevier.com/locate/seppur

Using eutectic solvents for extracting astaxanthin from dry biomass of *Xanthophyllomyces dendrorhous* pretreated by pulsed electric fields

Diego Artigas-Hernández [a,c], Alejandro Berzosa [b,c], Diederich Aguilar-Machado [b,c], Javier Raso [b,c], Manuela Artal [a,c,*]

[a] Departamento de Química Física, Facultad de Ciencias, Universidad de Zaragoza, Zaragoza, Spain
[b] Departamento de Ciencia y Tecnología de Alimentos, Universidad de Zaragoza, Zaragoza, Spain
[c] Instituto Agroalimentario de Aragón – IA2 (Universidad de Zaragoza – CITA), Zaragoza, Spain

ARTICLE INFO

Keywords:
Astaxanthin
Xanthophyllomyces dendrorhous
Pulsed electric fields
Hydrophobic eutectic solvents

ABSTRACT

The healthy properties of astaxanthin (AST) together with the growing interest in products of natural origin have motivated the development of sustainable extraction procedures from biomass. For this, it is essential to establish mechanisms that allow overcoming the barrier of the cell envelopes as well as the substitution of the conventional solvents. This work is focused on the evaluation of pulse electric fields (PEFs) as a fresh biomass pretreatment to enhance the efficacy of eutectic mixtures (ESs) as eco-friendly solvents for extracting AST from the freeze-dried yeast *Xanthophyllomyces dendrorhous*. The results showed a positive effect on the extraction efficiency of the pulse treatment and subsequent incubation stage. The thymol/salol system was the best solvent and the most favorable composition, temperature and extraction time were calculated. The efficiency reached 79% in the PEF-treated cells after incubation. The antioxidant capacity of AST in the eutectic mixture was determined and an IC_{50} value of 0.02 μg/mL was obtained. A synergistic effect between AST and thymol was observed. The main conclusion of the work is that consecutively using PEFs as an electroporation technique and ESs as solvents allows us to obtain a high extraction efficiency of AST from dry yeast.

1. Introduction

Carotenoids are compounds synthesized from 8 isoprene units that are classified into carotenes and xanthofhylls based on the absence or presence of oxygen in the molecule. Compared with carotenes which are molecules with only hydrocarbons, xanthophylls contain oxygen atoms in the form of a hydroxyl group or epoxides. The most important chemical feature of these compounds is the backbone of conjugated double bonds between two ring ends. The length of the chain and the presence of functional groups in both rings mark the properties of the carotenoids. Other influencing factors are isomerism and monomer aggregation. Several organisms such as bacteria, algae or fungi are able to synthesize carotenes by the addition of cyclases, hydroxylases, ketolases and other enzymes to the conjugated backbone. On the other hand, animals and humans must ingest them with food [1,2].

In this paper, astaxanthin (3,3′-dihydroxy-$\beta\beta'$-carotene-4,4′-dione, $C_{40}H_{52}O_4$) (AST) will be the carotenoid studied. Among the properties of AST, those related to health are the most notable. AST prevents age-related and cardiovascular diseases, and protects the skin from the sun. AST has antidiabetic and anticancer effect, and a high antioxidant capacity against free radicals [2].

AST belongs to the xanthophyll family with 13 conjugated double bonds and a hydroxyl and a ketone group adjoining in the ring ends. The most abundant geometrical isomers of AST are all-*trans*, 9-*cis*, 13-*cis*, and 15-*cis*. In addition, AST has two chiral carbons so it can exist in the form of two enantiomers, (3S,3′S) and (3R,3′R), and a *meso* form, (3R,3′S). Depending on the natural source, the optical isomer will be of one type or another. The (3S,3′S) isomer is the most abundant enantiomer in bacteria and algae and (3R,3′R) is the most abundant in yeast. A mixture of both isomers is found in crustaceans and all three forms are found in fish. The latter is because aquatic animals cannot synthesize AST. They obtain it from the chain food or as an additive in the form of synthetic AST whose composition contains the three isomers [3,4]. Moreover, AST molecules can be found free or as aggregates depending on the solvent. Two types of aggregates have been detected: the *H*-type (pack-of-card-arrangement) and the *J*-type (head to tail, linear arrangement) [5]. It is

* Corresponding author at: Departamento de Química Física, Facultad de Ciencias, Universidad de Zaragoza, Zaragoza, Spain.
E-mail address: martal@unizar.es (M. Artal).

https://doi.org/10.1016/j.seppur.2023.124496
Received 3 April 2023; Received in revised form 26 June 2023; Accepted 30 June 2023
Available online 1 July 2023

known that the different forms of AST have different biological activities. For instance, both enantiomers have higher antioxidant capacity than the *meso* form, and the aggregates have greater antioxidant capacity than free molecules. Additionally, *Z*-isomers present better bioavailability than *E*-isomers [6–8]. This structure of AST with a long conjugate chain and active groups has made it one of the healthiest carotenoids. Since it cannot be synthesized in animals, the AST market as a drug and nutraceutical is experiencing an exponential boom. Other industries such as dyes or cosmetics are contributing to this boom. Most commercial AST (95%) is of synthetic origin and its cost is much lower, between 2.5 and 7 times, that of natural sources. Despite this, the current trend in society promotes the constant increase in the consumption of natural AST. An overview of the production of AST can be found in the paper published by Aneesh et al. [2]. The main natural source of AST is the alga *Haematococcus pluvialis* whose extract has been approved by food agencies so it is commercialized as a food additive. The alga produces cysts filled with AST under stressed conditions such as malnutrition, high temperatures and luminous intensity. Its function is related to cellular protection and metabolism maintenance. The proportion of AST reported in this algae ranged from 30 to 70 g per kg of dry mass. It is fully in the form of the (3S,3′S) enantiomer and mostly (97%) esterified with fatty acids. The interest in the production of AST from *Xanthophyllomyces dendrorhous* an asexual reproductive stage of *Phaffia rhodozyma* has grown in recent years compared to that from algae. From *X. dendrorhous*, the AST form obtained is the (3R,3′R) enantiomer. The conditions for cultivation are easier and more flexible, and the use of genetic and metabolic engineering has provided mutations with high rates of AST yield. Several authors have achieved yields of up to 10 g/kg of dry biomass by applying extreme stress conditions on properly mutated strains. The yeast cell envelope consists of a distinct wall and a plasma membrane. While the wall is freely permeable to most molecules, the membrane exhibits selective permeability which makes it difficult to remove intracellular products such as AST that are typically biosynthesized and stored in yeast cells. Generally, the recovery of AST from *X. dendrorhous* is based on the use of several mechanical methods of cell disruption including bead mills, high-pressure homogenization or ultrasound in which the cells are broken down into fine particles during the prolonged disruption times required to maximize product recovery [9–12]. However, the intensity of this technique used for cell disruption results in the micronization of cell debris, having a negative impact on the subsequent purification of the desired product due to the increment in viscosity of the extract, the release of other compounds and the reduction of the efficiency of particulate removal during the subsequent centrifugation step [13]. Exposure of biological cells to pulsed electric fields (PEFs) causes an increase in their plasma membrane permeability thereby allowing for extraction of otherwise impermanent molecules [14]. This treatment which consists of the application of high-voltage, short-duration electric pulses permits the recovery of intracellular products without causing disruption of the cellular structure and therefore with a minimal micronization of cell debris. Recently, it was demonstrated that electroporation of *X. dendrorhous* cells by PEF followed by aqueous incubation permitted the subsequent extraction of AST from fresh biomass using ethanol as the solvent [15]. Other conventional organic solvents such as dimethyl sulfoxide or acetone are also used in the maceration of biomass but their environmental drawbacks are motivating the search for more sustainable solvents [2,16–18]. In addition, avoiding purification processes by designing formulations with solvents that enhance or complement the properties of AST could be a particularly interesting strategy. All this can be achieved using eutectic solvents (ESs) of tailor-made composition. The eutectic solvents are mixtures of substances whose melting temperature is lower than those of the pure compounds. The depression of the melting temperature is mainly a consequence of the establishment of a hydrogen bond network between the components. For this, they must be hydrogen bond donors (HBDs) or hydrogen bond acceptors (HBAs). Some compounds such as terpenes are able to act as HBDs or HBAs depending on the counterpart. The ESs are not chemically synthesized, so their preparation is simple and free of residues. Additionally, they have high stability, and are nonflammable and nonreactive with water. For all this, they are currently considered sustainable solvents with great potential for use in different applications [9–17]. A large number of eutectic mixtures can be prepared and those composed of substances of low toxicity are preferred. Moreover, if the components are active pharmaceutical ingredients such as terpenes and carboxylic acids, the eutectic mixtures obtained will be of special interest in biotechnology. In general, therapeutic ESs have hydrophobic character (hESs) so they present high affinity to nonpolar compounds and are good solvents in solid–liquid extractions [19–25]. Papers have been published on AST extraction with eutectic solvents but the combination of these solvents with PEF pretreatment to facilitate release has not been investigated [26–34].

The aim of this study was to evaluate if the electroporation by PEF of the fresh biomass of *X. dendrorhous* cells followed by an aqueous incubation enhanced the subsequent extraction of AST from the dried biomass using different hydrophobic eutectic solvents. To do this, an initial screening with seven terpene-based eutectic mixtures to choose the optimum solvent was performed. In the experiments, the effects of PEF and incubation treatment on the extraction efficiency of AST were evaluated. Second, the mole fraction of the optimum solvent, the temperature and the extraction time were optimized using response surface methodology (RSM). Finally, the antioxidant capacity of the extracted AST dissolved in the optimum solvent was measured.

2. Materials and methods

2.1. Chemicals

The chemicals (and their acronyms) used in this work were: thymol (T), menthol (M), salol (S), camphor (C), octanoic acid (O), decanoic acid (D), ethanol (EtOH), dimethyl sulfoxide (DMSO), *trans*-astaxanthin (tAST), and 2,2-diphenyl-1-picrylhydrazyl (DPPH). Table S1 (Supplementary Information) reports their characteristics and structures. They were used without further treatment.

2.2. Hydrophobic eutectic solvent preparation and characterization

The hydrophobic eutectic solvents (hESs) were prepared with the stirring and heating method. For that, the pure compounds were weighed in adequate proportions using a PB210S Sartorius balance (uncertainty $1{\cdot}10^{-4}$ g). Later, gentle heating to 50 °C and stirring were applied until a single liquid phase was obtained. The chosen composition of the mixtures was equimolar except for the menthol:camphor because the (1:1) ratio for this solvent was solid at 25 °C. Karl Fisher method with an automatic titrator Crison KF 1S-2B was used to measure the water content in hESs. The values were lower than 300 ppm for all mixtures.

Table 1 reports the acronyms used in the manuscript for these mixtures, the composition and density and dynamic viscosity at 25 °C. For the hESs not previously characterized, the properties were measured

Table 1
Characteristics of hESs mixtures: Acronym, composition, density (ρ), and viscosity (η) at 25 °C and 0.1 MPa.

Acronym	Compound 1	Compound 2	Molar ratio	ρ/kg/m^3	η/mPa·s
TO	Thymol	Octanoic acid	(1:1)	939.42[a]	9.201[a]
TM	Thymol	Menthol	(1:1)	932.93[b]	35.275[b]
TS	Thymol	Salol	(1:1)	1085.27	16.273
TC	Thymol	Camphor	(1:1)	966.98	20.817
MO	Menthol	Octanoic acid	(1:1)	901.09[c]	12.046[c]
M2C	Menthol	Camphor	(2:1)	912.41	21.359

[a] Ref. [35].
[b] Ref. [36].
[c] Ref. [37].

with an Anton Paar DSA 5000 vibrating tube densimeter and with a Schoot-Geräte AVS-440 viscometer. Both devices were thermostatically controlled ($u(T) = 0.01$ K) and tested by measuring the properties of benzene. The estimated uncertainties were: $U_c(\rho) = 0.05$ kg/m^3 and $U_c(\eta) = 1\%$ and the mean relative deviations in the checking were: *MRD* (ρ) = 0.004% and *MRD*(η) = 0.28%.

2.3. Biomass cultivation and treatment

2.3.1. Microorganism and cultivation conditions

Xanthophyllomyces dendrorhous ATCC® 74219™ was acquired from the American Type Culture Collection (ATCC, Beltsville, USA). The yeast strain and the inoculum were activated and prepared using the methodology previously described by Aguilar-Machado et al. [15]. Precultures were obtained by inoculating a single colony in a 100 mL Erlenmeyer flask with 25 mL of Potato-Dextrose Broth (PDB, Oxoid, Basingstoke, UK). The flask was then incubated at 25 °C for 2 days under agitation (270 xg) using an orbital shaker (Heidolph Unimax 1010, Germany). To produce AST, the inoculum with a cell density of approximately 10^6 cells/mL as determined by a Thoma counting chamber was cultivated at 25 °C in a 500 mL glass flask with 250 mL of PDB for 6 days under agitation (270*g*). The growth of yeast was monitored by measuring the cell density at 600 nm, the colony forming units per plate count (PDA, Oxoid, Basingstoke, UK), and carotenoid production.

2.3.2. PEF treatment

Before PEF treatment, the *X. dendrorhous* suspension was centrifuged at 4000*g* for 5 min at 4 °C using a Heraeus Megafuge 1.0R, (UK) to separate the supernatant and the fresh biomass was subsequently suspended in McIlvaine buffer (pH 7.0, 1.06 mS/cm) to a final concentration of $3{\cdot}10^{-3}$g dry weight/mL. PEF treatments were applied in a continuous flow by means of a commercial generator (Vitave, Pregue, Czech Republic) which has the ability to deliver pulses of 20 kV maximum voltage and 500 A. Square waveform monopolar pulses were delivered in parallel titanium electrode chambers with a 0.4 cm gap (3.0 × 0.5 cm) or 0.6 cm gap (5.0 × 0.6 cm). The actual voltage was measured using a high voltage probe (Tektronik, P6015A, Wilsonville, Oregon, USA) connected to an oscilloscope (Tektronik, TDS 220, Wilsonville, Oregon, USA). Yeast biomass was suspended in MacIlvaine buffer prepared from citric acid and disodium hydrogen phosphate. Both reagents were provided by Sigma-Aldrich and their purity was of 99%. The suspension was pumped (peristaltic pump, BVP, Ismatec, Wertheim, Germany) at a flow of 5 L/h through a parallel titanium electrode chamber with a 0.4 cm gap, 3 cm length and 0.5 cm width with a residence time of 0.44 s. Selected PEF treatment conditions were 50 square pulses of 3 μs pulse width and 8 kV/cm (63.67 kJ/kg) at a frequency of 15.7 Hz that electroporated >90% of the cells of *X. dendrorhous* [15].

After PEF treatment, the yeast suspension was divided into two aliquots. One aliquot was centrifuged at 4000*g* for 5 min at 4 °C and the pellet was frozen at −40 °C. The other aliquot was incubated in darkness for 24 h at 25 °C before centrifugation and subsequent freezing (−4 °C). To evaluate the effect of PEF treatments on the efficacy of eutectic solvents on the extraction of AST from dry biomass of *X. dendrorhous* the pellets of untreated cells (untreated), PEF-treated cells (PEF-treated), and PEF-treated cells after incubation (PEF-treated + incubation) were freeze-dried (FreeZone6, Labconco, Kansas City, USA) for 48 h and ground into a fine powder using a mortar and pestle. Hereinafter, the resulting pellets will be abbreviated in Figures and Tables as follows: untreated (*bU*), PEF-treated (*bPEF*), and PEF-treated + incubation (*bPEF + I*) biomass.

2.4. Extraction of AST from biomass

The total content of AST in the yeast was determined by solid–liquid extraction using DMSO. Previously, the cell wall was mechanically broken with bead-beating. A small mass (0.01 g) of each type of dry biomass (*bU, bPEF, bPEF + I*) was blended with 1 mL of DMSO. The yeast cells were disrupted using a bead beater (Bullet Blender Storm 24, Next advance, Troy, USA) with glass beads of 0.1 mm diameter at a speed of 4800 bpm until the pellets became colorless. Three cycles of 60 s were applied and the mixtures were cooled on ice after each beating cycle for 180 s.

In the extraction with hESs or EtOH, mixtures of 0.02 g of dry biomass and 5 mL of solvent were shaken with a magnetic stirrer inside an incubator at constant temperature. These values of the temperature and the extraction time depended on the conditions of each experiment which was replicated twice. All samples were analyzed after centrifugation (4000*g*) for 20 min.

2.5. AST analysis

A Waters Alliance 2695 HPLC equipped with a photodiode array detector Waters 2995 was used to obtain the profile of the extracts. Chromatographic separation was carried out in an ACE Excel 3 C18 super (3 μm, 150 × 4.6 mm) column, eluting isocratically with a mobile phase consisting of a mixture of methanol/dichloromethane/ acetonitrile/water (85.0:5.0:5.5:4.5, vol %) at 1 mL/min and 25 °C for 15 min. The extracts from biomasses *bU* and *bPEF* presented only one peak. By comparison with a standard sample, the retention time corresponded to *trans*-AST. The biomass *bPEF + I* showed a negligible second peak probably due to the cis isomer. Fig. S1 shows the HPLC chromatographic profile of the extractions with the TS mixture. Therefore, the samples were quantified by UV − vis spectroscopy using VWR 6300 PC double-beam equipment ($u(\lambda)$=±0.2 nm). The spectra from 400 to 600 nm were acquired, and the maximum absorbance was taken in the calculation. Fig. S2 displays the spectrum of the extract of *bPEF + I* sample in TS. For analysis of the total AST content, the following equation was used [15]:

$$W_{T,AST} = \frac{V \cdot A_{480} \cdot 10^9}{E^{1\%} \cdot 100 \cdot M} \quad (1)$$

where $W_{T,AST}$ is the AST yield (μg/g dry biomass); V is the solvent volume (mL); A_{480} is the absorbance at 480 nm; M is the dry biomass mass (g); and $E^{1\%}$ is the specific absorptivity of AST in DMSO (2100). For the solid–liquid extractions, calibration curves with synthetic AST and two solvents were prepared. In the initial screening with seven hESs, the calibration curve constructed from solutions of synthetic AST in EtOH at various concentrations (in parts per million, ppm_{AST}) was $A_{\lambda max} = 0.1795 \cdot ppm_{AST}$. To optimize the extraction conditions, TS diluted in EtOH (50:50, vol%) was used as the solvent and the equation was: $A_{\lambda max} = 0.2171 \cdot ppm_{AST} - 0.0071$. Each extraction was repeated three times and each sample was diluted in EtOH at three different proportions. Then, each result is the average of six analyses and is given with the confidence interval considering a 95% of confidence level. In this paper, they were expressed as extracted mass per gram of biomass (W_{AST}) or as extraction efficiency (EE_{AST}) related to the total content of AST in the yeast ($W_{T,AST}$):

$$EE_{AST} = 100 \frac{W_{AST}}{W_{T,AST}} \quad (2)$$

2.6. DPPH assay

The 2,2-diphenyl-1-picrylhydrazyl (DPPH) radical was used to determine the antioxidant capacity following the method developed by Blois [38]. The reduction reaction was monitored by UV − vis spectroscopy at λ = 517 nm and the concentration of the ethanolic DPPH solution was 0.08 mM. As a control, 0.2 mL of EtOH was mixed with 1.8 mL of the above solution and its absorbance was determined (A_C). For each sample to evaluate, several mixtures with similar amounts of sample in different EtOH volumes were prepared. The range of concentrations was chosen to give absorbance values within the sensitivity

range of the detector and follow the Lambert–Beer law: $0.3 < A_{517} < 0.8$ [39]. As blank, 0.2 mL of each sample was added to 1.8 mL of EtOH and its absorbance was measured (A_B). Finally, 0.2 mL of each sample was mixed with 1.8 mL of DPPH solution and stored in the dark. After 30 min of reaction time, the absorbance (A_S) was determined.

The inhibition percentage of DPPH (%In_{DPPH}) was calculated with Eq. (3). Usually, the antioxidant activity is given as the concentration required for the 50% inhibition of initial DPPH or half maximal inhibitory concentration (IC_{50}/(μg/mL)). For that, linear equations of %In_{DPPH} versus final concentration of mixtures (Q_S/(μg/mL)) were fitted (Eq. (4)). The equations are:

$$\%In_{DPPH} = \frac{A_c - (A_s - A_B)}{A_c} \quad (3)$$

$$\%In_{DPPH} = A + BQ_S \quad (4)$$

2.7. Statistical analysis

To optimize the extraction conditions with the optimal solvent, an experimental central composite design (CCD) was performed using Design Expert 13 Ver. 22.0.2 (Stat-Ease Inc., Minneapolis, MN, USA) with three variables. Seventeen randomized runs with three center points were conducted and the response surface methodology (RSM) approach was used to determine the effect of the parameters. The following equation (quadratic model) was used to correlate the results and to obtain the best extraction conditions:

$$Y = \beta_0 + \sum_{i=0}^{3} \beta_i X_i + \sum_{i=0}^{3} \sum_{j=0}^{3} \beta_{ij} X_i X_j \quad (5)$$

where Y is the response; X_i and X_i are the independent variables; β_0 and β_i are the intercept and the linear regression coefficients, respectively; and β_{ij} indicates the crossing ($i \neq j$) and the quadratic ($i = j$) coefficients.

The experimental data were evaluated statistically by the software with an analysis of variance (ANOVA) confirming the significance of the regression model; the F test was performed using a 95% ($\alpha = 0.05$) level of significance. The model was checked by comparing the predicted and experimental data. Each experiment was performed in triplicated and each result was the mean of at least six analyses.

3. Results and discussion

3.1. Extraction of AST from PEF-treated X. dendrorhous freeze-dried biomass using different eutectic solvents

3.1.1. Effect of PEF on the extraction of AST from X. dendrorhous freeze-dried biomass

To evaluate the effect of PEF on the extraction of AST from freeze-dried biomass of *X. dendrorhous* by the hydrophobic eutectic solvents shown in Table 1, a preliminary extraction trial was conducted at 25 °C for 6 h. Fig. 1a shows the extraction yield expressed as a percentage of AST extracted from freeze-dried biomass of untreated (*bU*), PEF-treated (*bPEF*) and PEF-treated + incubation (*bPEF + I*) cells. The extract obtained using EtOH as a control solvent is also shown in the figure. With the exception of M2C, MO and TO mixtures, hESs exhibited a higher efficiency than EtOH for the three biomasses. Table S2 reports the total amount of extracted AST expressed as μg of AST per g of dry biomass and the percentage of AST extracted with respect to the total content in the biomass calculated by extracting with DMSO from the bead-beaten biomass ($W_{T,AST}$ = 3172 $\mu g_{AST}/g_b$).

Fig. 1a shows that the extraction efficiency (EE_{AST}), calculated with Eq. (2), of the different solvents was higher in the biomass that was treated by PEF before freeze drying as compared with the untreated biomass. The improvement in the extraction of different intracellular compounds from both plant and microbial cells when the cytoplasmic membrane has been previously electroporated by PEF has been reported by different authors [40]. This effect is attributed to the fact that the selective permeability of the phospholipid bilayer is lost leading to the leakage of the compounds located in the cytoplasm. It has been demonstrated that when compared with untreated cells, this effect not only speeds up the extraction of intracellular compounds but also permits obtaining higher extraction yields. Generally, in studies on the extraction of intracellular compounds assisted by PEF both PEF treatment and subsequent extraction have been conducted with fresh biomass. The results obtained in our investigation demonstrated the benefits in terms of improving extraction yield derived from the increment of the permeability of the cell membrane as a consequence of the application of PEF. This was also observed when the extraction was conducted from dried biomass of *X. dendrorhous* that was treated by PEF before freeze-drying. The removal of water from the cells of the yeast by freeze-drying permitted the access of hydrophobic eutectic solvents that are required to extract compounds of hydrophobic nature located in the cytoplasm such as AST. Fig. 1a also shows that an aqueous incubation of the PEF treated fresh biomass for 24 h made the extraction of AST more efficient for all the eutectic solvents investigated. The amount of

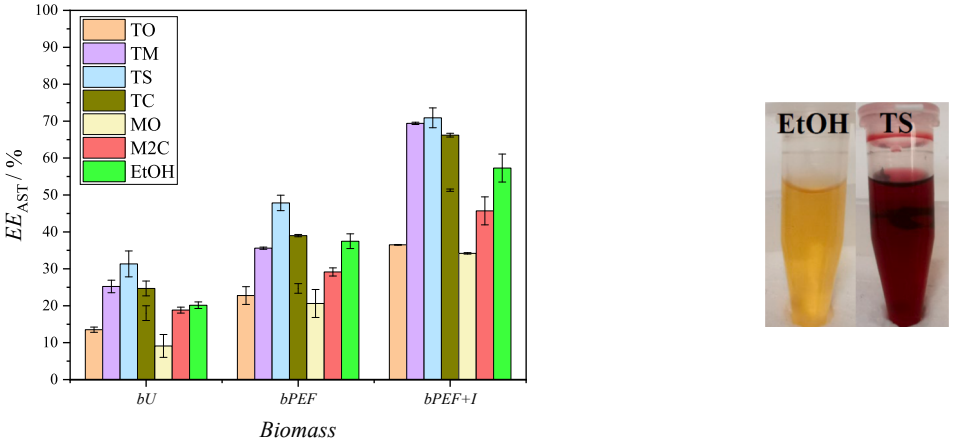

Fig. 1. (a) Extraction efficiency of AST from freeze-dried untreated (*bU*), PEF treated (*bPEF*) and PEF treated after incubation (*bPEF + I*) biomass of *X.* after 6 h of extraction at 25 °C using EtOH and different eutectic solvents. TO, TM, TS, TC, MO, M2C, EtOH. Error bars, 95% CI. (b) Color of the extraction medium after extracting AST from *bPEF + I* biomass in EtOH and in TS.

extracted AST from the PEF-treated + incubation biomass was 50–100% higher than that in the PEF-treated and nonincubated biomass. Aguilar-Machado et al. [15] demonstrated that the extraction of AST from fresh biomass using EtOH as solvent was only effective after aqueous incubation of PEF-treated cells for a period of time. In this case, the value of the extraction efficiency was of 70%. The detection of esterase activity in the supernatant during incubation and the existence of a relationship between the percentage of esterase activity and the amount of AST extracted in the subsequent extraction seemed to indicate that esterase activity triggered by PEF mediated the effective ethanolic extraction of AST. It was hypothesized that uncontrolled molecular transport through the electroporated cytoplasmic membrane of yeast decreases the osmotic pressure of the cytoplasm. This fact causes plasmolysis of the lysosomes and the release of esterases that hydrolyze the triacylglycerides of the lipid droplets. The loss of structure in hydrolysis allows the release of carotenoids located in the droplets. Consequently, once the carotenoids are free in the cytoplasm, they are more accessible for the extraction solvents facilitating the formation of the carotenoid-solvent complex that diffuses across the cell membrane driven by a concentration gradient.

3.1.2. Influence of composition of eutectic solvents on extraction of AST from X. dendrorhous freeze-dried biomass

Fig. 1a shows that the extraction profile of the different solvents assayed was similar for the three *X. dendrorhous* biomasses evaluated. In both eutectic solvents containing thymol or menthol the combination with octanoic acid results in a less effective solvent. In the best scenario that corresponded to the extraction conducted from the PEF-treated + incubation biomass, the extraction efficiency obtained with the solvents containing octanoic acid was lower than 40%. This effect could be explained by the fact that the acidity provided by the carboxylic acids impaired AST solubilization. On the other hand, eutectic solvents containing thymol were more effective than those that contained menthol for the three biomasses studied. The highest extraction yield with the M2C mixture was approximately 45% and with the three solvents containing thymol, it was 65–70% of the total content. This fact highlights the importance of π–π interactions between the aromatic rings of thymol and those of AST. In all cases, the maximum values were obtained from the PEF-treated biomass that was incubated before freeze-drying. A higher EE_{AST} of thymol-based eutectic mixtures was already observed by Pitacco et al. [28]. No-statistically significant differences ($p > 0.05$) were observed in the efficiency of extraction from the PEF-treated + incubated biomass using TM, TS, and TC mixtures as solvents. Conversely, TS was the best solvent to extract AST from the untreated and PEF-treated biomass. The combination of high density and low viscosity of TS (Table 1) facilitates access of this solvent to lipid droplets containing AST in yeast cells.

In addition to the good properties of TS for the extraction of AST from the different biomasses tested, the AST dissolved in this mixture presented high stability over time. The concentration of AST decreased by less than 5% after 42 h at 25 °C in this eutectic solvent (Table S2). Finally, the redshift observed in the spectra of the AST extracted in the TS solvent is remarkable (Table S2, Fig. 1b). This effect is related to the formation of *J*-type loosely packed aggregates [7,41]. The strong interaction between the conjugated diene of AST and the π-rings of salol could be the cause of this preferential orientation. The presence of aggregates affects AST properties, and specifically, those of the *J*-type are especially interesting for using carotenoids as colorants [42]. Consequently, in the next step aiming to optimize the extraction of AST from the three available freeze-dried biomasses of *X. dendrorhous*, the eutectic TS was selected.

3.2. Evaluation of the extraction conditions of AST from X. dendrorhous freeze-dried biomass using the best solvent

Once the thymol/salol eutectic system was selected as solvent, several experiments were performed to obtain the best extraction conditions. The three variables evaluated were the thymol mole fraction in the optimum solvent (x_T), the temperature (T) and the extraction time (t). They were chosen so that the mixtures were liquid in the widest possible temperature range, avoiding both thermal and temporal decomposition of the AST. The characteristics of each trial proposed by the CCD design and the experimental results are listed in Table 2. The extraction conditions had more influence on the untreated biomass than on the others biomasses. First, the value of the amount extracted was doubled depending on the conditions. The increase for the PEF-treated and PEF-treated + incubated biomasses was 50% and 30%, respectively. Considering the total amount of extracted AST ($W_{T,AST} = 3172\ \mu g_{AST}/g_b$), the maximum extraction efficiency from each type of biomass was: $EE_{AST}(bU) = 55\%$, $EE_{AST}(bPEF) = 65\%$, and $EE_{AST}(bPEF + I) = 79\%$. It should also be noted that in most of the x_T and T conditions, the mass extracted from *bPEF* + *I* biomass after 4 h of extraction time was greater than that obtained for the *bU* and *bPEF* after 24 h. These values highlighted the importance of both pulsed electric field and incubation treatments to improve the extraction process as seen above in Section 3.1. The experimental data were analyzed and fitted by the mathematical model to obtain the regression coefficients of Equation (5). After eliminating the nonsignificant parameters ($p > 0.1$), the extracted mass of AST per gram of biomass, $W_{AST}(\mu g_{AST}/g_b)$, for the untreated (*bU*), PEF-treated (*bPEF*), and PEF-treated + incubation (*bPEF* + *I*) biomasses can be calculated as follows (actual factors):

Table 2
Extraction efficiency of AST from freeze-dried untreated (*bU*), PEF treated (*bPEF*) and PEF treated after incubation (*bPEF* + *I*) biomass of *X. dendrorhous* according to the thymol/salol mole fraction (x_T), temperature (T) and extraction time (t). Matrix established by central composite design (CCD) and the results are presented in terms of extracted mass of AST per gram of dry biomass (W_{AST}). *

Mole fraction, x_T	Temperature T/°C	Extraction time t/h	W_{AST}/(μg/g dry biomass)		
			bU	*bPEF*	*bPEF* + *I*
0.3	20	4	1374 ± 21	1546 ± 22	1920 ± 26
0.5	20	4	916 ± 23	1361 ± 28	1866 ± 14
0.3	40	4	1047 ± 24	1592 ± 27	2214 ± 14
0.5	40	4	1246 ± 17	1541 ± 22	2136 ± 20
0.3	20	24	1866 ± 7	2080 ± 16	2410 ± 18
0.5	20	24	1569 ± 30	1880 ± 27	2380 ± 25
0.3	40	24	1765 ± 27	2114 ± 33	2506 ± 21
0.5	40	24	1547 ± 27	1947 ± 39	2520 ± 34
0.3	30	14	1494 ± 15	1842 ± 11	2194 ± 18
0.5	30	14	1419 ± 11	1886 ± 16	2200 ± 22
0.4	20	14	1399 ± 12	1755 ± 23	2284 ± 49
0.4	40	14	1374 ± 24	1740 ± 25	2290 ± 20
0.4	30	4	996 ± 24	1379 ± 40	1893 ± 43
0.4	30	24	1393 ± 30	1926 ± 15	2506 ± 14
0.4	30	14	1445 ± 36	1844 ± 21	2180 ± 19
0.4	30	14	1426 ± 17	1774 ± 27	2159 ± 18
0.4	30	14	1502 ± 14	1848 ± 9	1999 ± 7

* Mean ± 95% confidence interval.

$$W_{AST}(bU) = 3225.56–11364.47{\cdot}x_T + 62.17{\cdot}t + 13144.34{\cdot}x_T^2–1.31{\cdot}t^2 \quad (6)$$

$$W_{AST}(bPEF) = 2848.03–7711.45{\cdot}x_T + 59.47{\cdot}t + 8940.57{\cdot}x_T^2–1.22{\cdot}t^2 \quad (7)$$

$$W_{AST}(bPEF + I) = 1665.80 + 8.06{\cdot}T + 22.93{\cdot}t \quad (8)$$

Table 3 shows the ANOVA treatment of the model, whose parameters were within of the recommended values. The model was significant for the three types of biomasses with p values of each coefficient lower than 0.0001 and F values higher than 12. Additionally, the F value of each variable is related to its weight in the model. The higher the F value is, the higher the importance. For all cases, the extraction time was the most influential factor. Other statistical parameters indicative of the adequacy of the model are: a signal-to-noise ratio (adequate precision) higher than 4, a high regression coefficient, and a difference between the adjusted and predicted coefficients of regression lower than 0.2. In this work, the results obtained meet all these requirements, as shown in Table 4.

A graphical diagnosis of the model can be performed with the actual and residual responses against the predicted response. Fig. S3 shows this information for our data. In addition, several randomly chosen confirmation points were determined and compared with those predicted (Table S3). The deviations ranged from 0.1% to 4%.

To illustrate the influence of the three factors studied on the extraction efficiency, graphical representations using the mathematical model (Eqs. (6)–(8)) were obtained. Fig. 2 shows that the influence of the three variables on AST extraction from the PEF-treated + incubation (*bPEF + I*) biomass was different than from the untreated (*bU*) and PEF-treated (*bPEF*) biomasses. For the first, AST extraction was independent of the thymol mole fraction and was a function of the linear terms of time and temperature. For the other biomasses, AST extraction was independent of the temperature and was a function of the lineal and quadratic terms of thymol mole fraction and time. Fig. 2a shows the effect of the thymol mole fraction (x_T) at $T = 20$ °C and $t = 24$ h. The extracted AST from untreated (*bU*) and PEF + treated (*bPEF*) biomasses decreased showing a slight minimum and that from the PEF-treated + incubation (*bPEF + I*) was independent of the composition. Fig. 2b shows the effect of the temperature at $x_T = 0.3$ and $t = 24$ h. T was not a significant factor in the extraction from untreated *bU* and *bPEF* biomasses. On the other hand, the W_{AST} increased linearly with T by a 4% in the extraction from *bPEF + I*. Fig. 2c displays that the extraction time at $x_T = 0.3$ and $T = 20$ °C was the most significant factor for all types of biomasses, showing a linear relationship in *bPEF + I*. The higher the extraction time, the higher the efficiency. Under these x_T and T conditions, the W_{AST} extracted from *bPEF + I* biomass after an extraction time of 4 h was similar to that obtained from *bPEF* at $t = 13$ h and was higher than that extracted from *bU* at $t = 24$ h. The different influence of factors on AST extraction may be related to the fact that, unlike to *bU* and *bPEF* cells, AST in *bPEF + I* is free in the cytoplasm. For the former, the interaction between AST and lipids would hinder the dissolution of the carotenoid in the eutectic system.

Table 3
ANOVA results of the models for untreated (*bU*), PEF-treated (*bPEF*), and PEF-treated + incubation (*bPEF + I*) biomasses.

Biomass	Variables	Sum of squares	df	Mean square	F-value	*p*-value
bU	Model	7.966E+05	4	1.991E+05	13.94	0.0002
	A–x_T	72080.10	1	72080.10	5.04	0.0443
	C–*t*/h	6.559E+05	1	6.559E+05	45.89	<0.0001
	A^2	52325.74	1	52325.74	3.66	0.0798
	C^2	51622.08	1	51622.08	3.61	0.0816
	Residual	1.715E+05	12	14290.82		
	Lak of Fit	1.686E+05	10	16858.92	11.62	0.0818
	Pure error	2900.67	2	1450.33		
	Cor Total	9.681E+05	16			
bPEF	Model	7.184E+05	4	1.796E+05	43.50	<0.0001
	A–x_T	31248.10	1	31248.10	7.57	0.0176
	C–*t*/h	6.391E+05	1	6.391E+05	154.79	<0.0001
	A^2	24208.50	1	24208.50	5.86	0.0322
	C^2	45147.00	1	45147.00	10.94	0.0063
	Residual	49542.83	12	4128.57		
	Lak of Fit	46078.83	10	4607.88	2.66	0.3040
	Pure error	3464.00	2	1732.00		
	Cor Total	7.679E+05	16			
bPEF + I	Model	5.907E+05	2	2.954E+05	56.40	<0.0001
	B–*T*/°C	64963.60	1	64963.60	12.40	0.0038
	C–*t*/h	5.258E+05	1	5.258E+05	100.39	<0.0001
	Residual	68083.25	13	5237.17		
	Lak of Fit	67862.75	12	5655.23	25.65	0.1532
	Pure error	220.50	1	220.50		
	Cor Total	6.588E+05	15			

Table 4
Fit statistics of the regression model for untreated (*bU*), PEF-treated (*bPEF*), and PEF-treated + incubation (*bPEF + I*) biomasses.

	bU	*bPEF*	*bPEF + I*
Std. Dev.	119.54	64.25	72.37
Mean	1397.82	1767.94	2228.63
C.V./%	8.55	3.63	3.25
R^2	0.8229	0.9355	0.8967
R^2_{adj}	0.7638	0.9140	0.8808
R^2_{pred}	0.6079	0.8587	0.8402
Adeq. Precision	11.2374	18.6792	19.7789

The extension of this study to any condition within the studied ranges can be performed with 3D surface plots which allow us to analyze the mutual interactions between the factors. In Fig. 3, these graphs were obtained by fixing the least significant parameter to the central value (maybe not optimal) which was $T = 30$ °C for *bU* and *bPEF* and $x_T = 0.4$ for *bPEF + I*. The results presented previously in which the t factor exhibited the highest slope were confirmed in all cases. The noncircular 2D contour plots indicated the nonsignificance of the mutual interaction factors. In the model, the p values of the crossing coefficients ($x_T{\cdot}t$), ($x_T{\cdot}T$), and ($T{\cdot}t$), were higher than 0.1 for the three types of biomasses. In addition, a curved relationship between the two significant factors was obtained in the results corresponding to the biomass of *bU* and *bPEF* and a linear relationship for those of *bPEF + I*.

The desirability function is a method widely used in industry to optimize a process that depends on multiple variables. According to this approach, a process that depends on several factors is acceptable if each of these factors is within the desired limits. It ranges from 0 for a completely undesirable value to 1 for an ideal value. In this work, two types of calculations were made. First, the W_{AST} was maximized for any value of the three factors within the working range, obtaining the highest value of desirable function. For all biomasses, the most favorable x_T was the one most concentrated in salol and the best t matched the maximum in the worked range. The first fact could be due to the higher ability of this compound to establish π-interactions with AST and the second result would be related to the time required to establish the carotenoid-solvent complex. The values of the desired function for *bU*, *bPEF*, and *bPEF + I* were 0.87, 0.93 and 1, respectively. Table 5 lists the extraction conditions, and the predicted and actual responses. The deviations between the latter ranged from 0.1 to 1.6%. Second, the maximal W_{AST} was calculated minimizing the extraction time. This t_{min} was approximately 10 h in all cases and, again, the best composition was $x_T = 0.3$. As expected, the desirable functions in this calculation were less than those above: 0.65, 0.65 and 0.61. Fig. S4 displays the 3D–plots of the desirability function for the three types of biomasses. The deviations between the predicted and actual responses (Table 5) ranged from 0.6% to 3%. The most favorable extraction conditions for minimizing the temperature were $x_T = 0.3$ and $t = 24$ h and the W_{AST} values are shown and discussed above (Table 2).

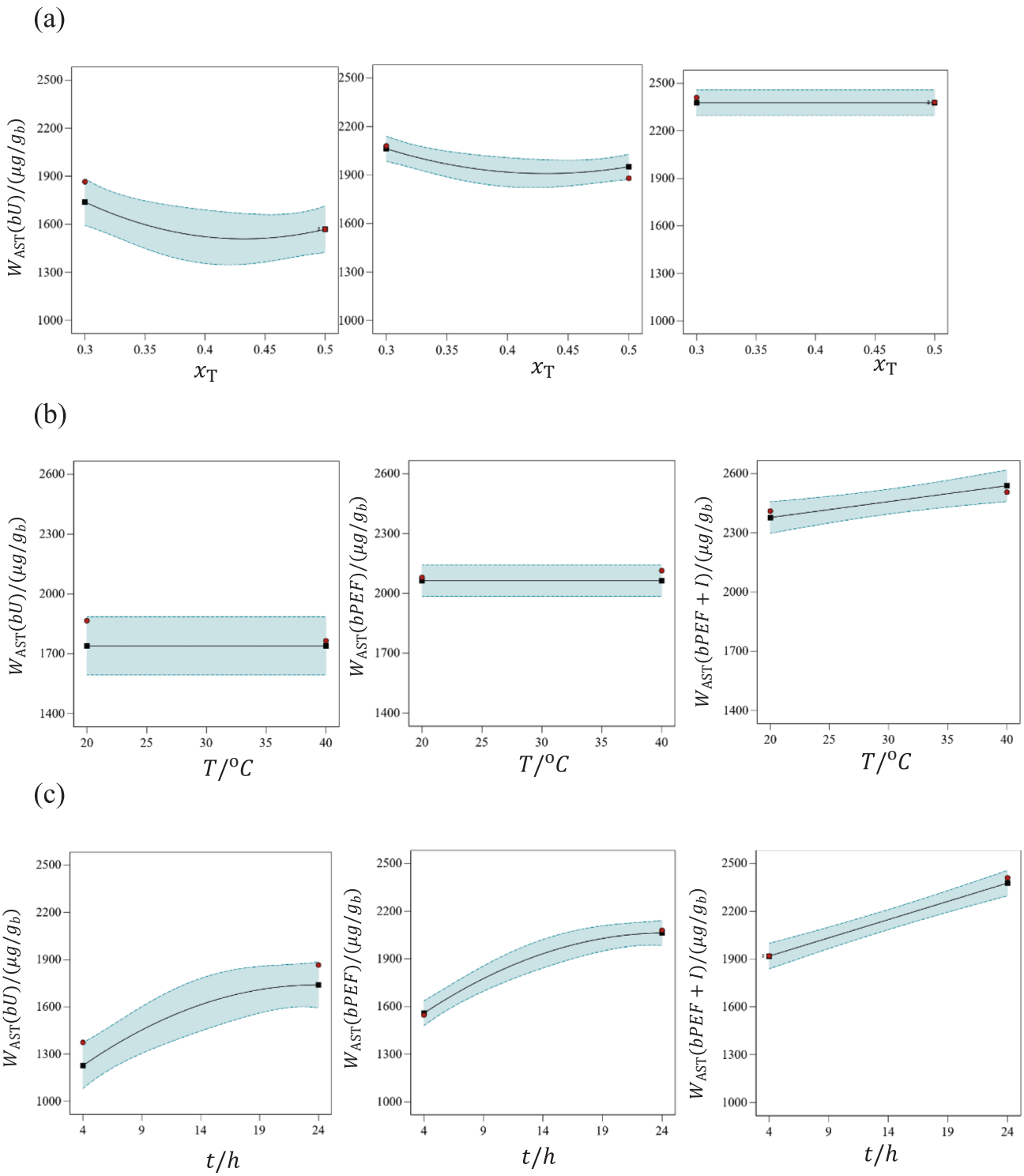

Fig. 2. Extracted mass of AST per gram of biomass, W_{AST}/(μg/g biomass), from freeze-dried untreated (*bU*), PEF treated (*bPEF*) and PEF treated after incubation (*bPEF* + *I*) biomass of *X*. Effect of different factors on the efficiency extraction: (a) Effect of the thymol mole fraction (x_T) at $T = 20$ °C and $t = 24$ h; (b) Effect of the temperature (T) at $x_T = 0.3$ and $t = 24$ h; (c) Effect of the extraction time (t) at $x_T = 0.3$ and $T = 20$ °C. (●), experimental point; (–) and (■), mathematical model; (▒), ±95% confidence interval bands.

3.3. Antioxidant activity

The pharmacological properties of thymol, salol and AST are well known [2,43,44] so a joint formulation of the three compounds could be of interest. One of the most important applications of AST comes from its ability to act as an antioxidant agent against free radicals. In this section, the antioxidant capacity of AST extracted with the thymol/salol mixture at a concentration of $x_T = 0.3$ was evaluated. For this, the inhibition percentage of DPPH (Eq. (3) and the half maximal inhibitory concentration (IC_{50}) of various samples were obtained. Table 6 shows the IC_{50} experimental values from this work and those found in the literature. The fitted and regression coefficients of the equation used to calculate them (Eq. (4)) are listed in Table S3. According to its definition (Section 2.6), the higher the IC_{50} value is, the lower the antioxidant activity. The

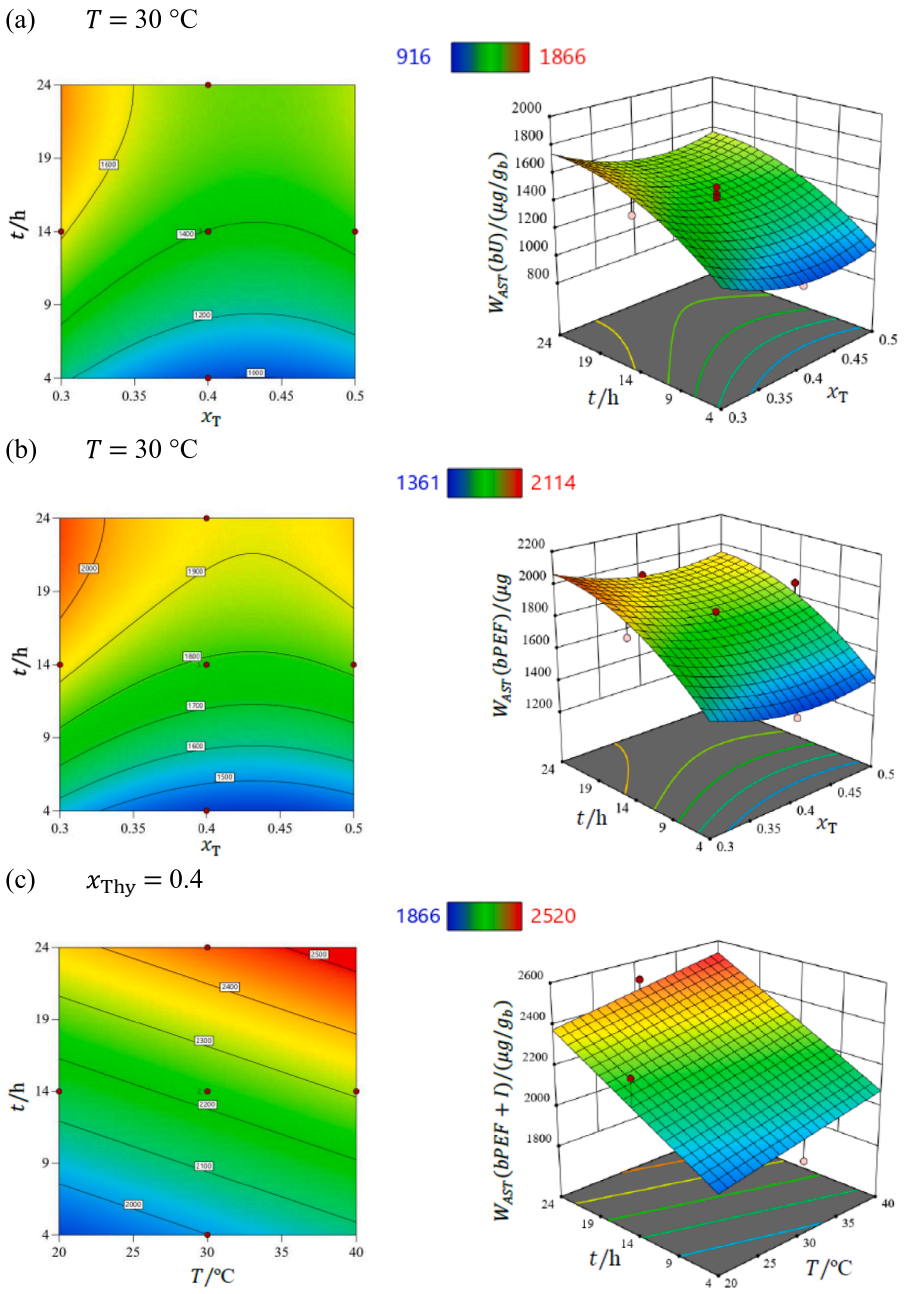

Fig. 3. Response 2D–contour and 3–D surface plots representing the interaction effect between the two more significant factors with the third one being constant and equal to the central value. Extracted mass of AST per gram of biomass, W_{AST}/(μg/g biomass), from the three types of biomasses of *X.* (a) freeze-dried untreated (*bU*), (b) PEF treated (*bPEF*), and (c) PEF treated after incubation (*bPEF* + *I*).

results of the DPPH assay strongly depend on the procedure used to obtain them [39,46,47]. The concentration of the reactive species, the nature of the solvent, and the reaction time must be established to be able to compare the values obtained. To check the procedure, the measurement of the antioxidant activity of a sample considered as a reference standard is recommended. We used ascorbic acid and the IC_{50} data found in the literature ranged from 1.80 to 111 μg/mL [47]. Our value was in good agreement with several of them (Table 6), including the one determined by Deutchoua et al. [45] with the electrochemical method. To study the potential synergistic effect between AST and the solvent, the antioxidant activity of thymol, salol, the best eutectic mixture, and AST was determined. The thymol exhibited a moderate antioxidant capacity and the value was close to that published by Beena et al. [48]. No antioxidant capacity was shown for salol. For the solvent (thymol/salol with $x_T = 0.3$), the IC_{50} value was 2.5 times that of pure thymol, which was close to the stoichiometric ratio of thymol in the mixture. In addition, the inhibition coefficient of the solution of the standard AST in the most favorable solvent was much lower than that obtained using DMSO as the solvent. This fact confirmed the positive synergistic effect of thymol. Some authors explain the high antioxidant capacity of AST as a consequence of the equilibrium established with the enol form of the ketone whose extension depends on the solvent. The conjugated *ortho*-dihydroxy-polyene formed has a high capacity to donate protons [50,51]. Furthermore, a higher antioxidant capacity of AST in the aggregate form was observed by Dai et al. [7]. Both the formation of hydrogen bonds and the increase in the conjugated π–π structure in the aggregates enhance the transfer of hydrogen to the radicals. All this was favored by the presence of solvents such as thymol (Section 3.1). Finally, to compare the activity of synthetic versus natural AST, the IC_{50} of extracted AST with the thymol/salol mixture ($x_T = 0.3$)

Table 5
Extraction efficiency of AST in terms of extracted mass of AST per gram of dry biomass (W_{AST}) from freeze-dried untreated (*bU*), PEF treated (*bPEF*) and PEF treated after incubation (*bPEF + I*) biomass of *X. dendrorhous*. The results according to the most favorable conditions with all factors in range, and minimizing the extraction time with mole fraction and temperature in range.

				W_{AST}/(μg/g dry biomass)			
	Variables			Predicted			Actual*
Biomass	x_T	T/°C	t/h	95% CI low	Mean	95% CI high	
All factors in range							
bU	0.3	37.3	23.8	1595	1739	1883	1737 ± 12
bPEF	0.3	20.0	24.0	1985	2063	2142	2043 ± 16
bPEF + I	0.3	39.4	23.8	2453	2532	2611	2497 ± 13
Minimum t; x_T and T in range							
bU	0.3	32.9	9.4	1324	1467	1628	1422 ± 33
bPEF	0.3	27.2	10.4	1741	1825	1909	1877 ± 47
bPEF + I	0.3	40	9.3	2142	2202	2275	2188 ± 44

* Mean ± 95% confidence interval.

Table 6
Results of the antioxidant capacity presented in terms of half maximal inhibitory concentration (IC_{50}).

Sample	IC_{50}/(μg/mL)
Ascorbic acid	3.23/4.46[a]/2.52[b]/4.58[c]/2.08[d]/1.80[e]
Thymol	153.3/167.57[f]
TS (1:2)	397.7
AST standard	12.32/11.13[g]
AST standard in TS (1:2)	0.07
AST extracted in TS (1:2)	0.015

[a] Ref. [45].
[b] Ref. [52].
[c] Ref. [53].
[d] Ref. [54].
[e] Ref. [47].
[f] Ref. [48].
[g] Ref. [49].

was determined and compared with the abovementioned results using standard AST. The value was 3.5 times lower than that of the synthetic compound, which is equivalent to a higher antioxidant activity. This result may be related to the different contents of isomers in both samples. The literature reports that the antioxidant activity of the major isomer in *X. dendrorhous* (3R,3′R) is higher than that of the *meso* form of synthetic AST [51].

4. Conclusions

In this study, the extraction of AST from *X. dendrorhous* was performed. For this purpose, PEF treatment was applied to electroporate the cytoplasmic membrane and several eutectic mixtures were used as eco-friendly solvents. The experiments were performed with three different types of freeze-dried biomasses: untreated (*bU*), PEF-treated (*bPEF*), and PEF-treated + incubation (*bPEF + I*). Therefore, the effects of PEF and the extraction conditions could be evaluated. The results were analyzed with the response surface methodology approach and the best extraction conditions were calculated. The factors studied were solvent composition, temperature, and extraction time. In addition, the antioxidant activity of the extracted AST was measured. All results showed the positive effect of PEF especially when the cells were incubated for 24 h before freeze drying. From the screening experiments, the thymol/salol system was chosen as the most appropriate solvent. The extraction efficiency reached 71% for the *bPEF + I* sample. The analysis of the extraction conditions indicated that the maximum AST mass for all biomasses could be extracted under the following operational conditions: $x_T = 0.3$, and $t = 24$ h. The actual values of efficiency were: $EE_{AST}(bU) = 55\%$, $EE_{AST}(bPEF) = 65\%$, and $EE_{AST}(bPEF + I) = 79\%$. The efficiency decreased in the most favorable composition and temperature conditions, and minimum extraction time ($t_{min} = 10$ h) with the values: $EE_{AST}(bU) = 45\%$, $EE_{AST}(bPEF) = 59\%$, and $EE_{AST}(bPEF + I) = 69\%$. Finally, an extremely high antioxidant capacity of the extracted AST in the thymol/salol ($x_T = 0.3$) mixture was observed. In the DPPH test, an IC_{50} value of 0.02 μg/mL was obtained.

We proposed the possible use as it is of the liquid mixture containing AST extracted from a natural source as solute and a mixture of active principles as solvent. It is known that *X. dendrorhous* provides, especially under stress conditions, a high proportion of AST (95% of the carotenoids produced). In addition, active principles such as thymol and salol could increase the benefits of the use of AST as an additive or drug. For all this, purification and separation stages were not evaluated in this paper and these questions could be proposed as outlook in this line of research.

CRediT authorship contribution statement

Diego Artigas-Hernández: Conceptualization, Formal analysis, Data curation. **Alejandro Berzosa:** Formal analysis, Data curation. **Diederich Aguilar-Machado:** Conceptualization. **Javier Raso:** Supervision, Funding acquisition, Writing – original draft, Writing – review & editing. **Manuela Artal:** Conceptualization, Supervision, Writing – original draft, Writing – review & editing.

Declaration of Competing Interest

The authors declare that they have no known competing financial interests or personal relationships that could have appeared to influence the work reported in this paper.

Data availability

All data are reported in the Supplementary file

Acknowledgments

This research was supported by the IA2 (LTIA20125-01). PLATON research group acknowledges financial support from Gobierno de Aragón and Fondo Social Europeo “Construyendo Europa desde Aragón” E31_23R.

Appendix A. Supplementary material

Supplementary material to this article can be found online at https://doi.org/10.1016/j.seppur.2023.124496.

References

[1] V. Ashokkumar, G. Flora, M. Sevanan, R. Sripriya, W.H. Chen, J.H. Park, J. Rajesh Banu, G. Kumar, Technological advances in the production of carotenoids and their applications– A critical review, Bioresour. Technol. 367 (2023), https://doi.org/10.1016/j.biortech.2022.128215.
[2] P.A. Aneesh, K.K. Ajeeshkumar, R.G.K. Lekshmi, R. Anandan, C.N. Ravishankar, S. Mathew, Bioactivities of astaxanthin from natural sources, augmenting its biomedical potential: A review, Trends Food Sci. Technol. 125 (2022) 81–90, https://doi.org/10.1016/j.tifs.2022.05.004.
[3] W. Yu, J. Liu, Astaxanthin isomers: Selective distribution and isomerization in aquatic animals, Aquaculture 520 (2020), 734915, https://doi.org/10.1016/j.aquaculture.2019.734915.
[4] V.M. Moretti, T. Mentasti, F. Bellagamba, U. Luzzana, F. Caprino, G.M. Turchini, I. Giani, F. Valfrè, Determination of astaxanthin stereoisomers and colour attributes in flesh of rainbow trout (*Oncorhynchus mykiss*) as a tool to distinguish the dietary

pigmentation source, Food Addit. Contam. 23 (2006) 1056–1063, https://doi.org/10.1080/02652030600838399.
[5] G. Britton, S. Liaaen-Jensen, H. Pfander, Carotenoids, Birkhäuser Verlag, Basel – Boston - Berlin, n.d.
[6] C. Yang, H. Zhang, R. Liu, H. Zhu, L. Zhang, R. Tsao, Bioaccessibility, Cellular Uptake, and Transport of Astaxanthin Isomers and their Antioxidative Effects in Human Intestinal Epithelial Caco-2 Cells, J. Agric. Food Chem. 65 (2017) 10223–10232, https://doi.org/10.1021/acs.jafc.7b04254.
[7] M. Dai, C. Li, Z. Yang, Z. Sui, J. Li, P. Dong, X. Liang, The astaxanthin aggregation pattern greatly influences its antioxidant activity: A comparative study in CACO-2 cells, Antioxidants 9 (2020), https://doi.org/10.3390/antiox9020126.
[8] M. Honda, K. Murakami, Y. Osawa, Y. Kawashima, K. Hirasawa, I. Kuroda, Z-Isomers of Astaxanthin Exhibit Greater Bioavailability and Tissue Accumulation Efficiency than the All- E-Isomer, J. Agric. Food Chem. 69 (2021) 3489–3495, https://doi.org/10.1021/acs.jafc.1c00087.
[9] M. Hasan, M. Azhar, H. Nangia, P.C. Bhatt, B.P. Panda, Influence of high-pressure homogenization, ultrasonication, and supercritical fluid on free astaxanthin extraction from β-glucanase-treated *Phaffia rhodozyma* cells, Prep. Biochem. Biotech. 46 (2016) 116–122, https://doi.org/10.1080/10826068.2014.995807.
[10] R.K. Saini, Y.-S. Keum, Carotenoid extraction methods: A review of recent developments, Food Chem. 240 (2018) 90–103, https://doi.org/10.1016/j.foodchem.2017.07.099.
[11] L. Urnau, R. Colet, V.F. Soares, E. Franceschi, E. Valduga, C. Steffens, Extraction of carotenoids from *Xanthophyllomyces dendrorhous* using ultrasound-assisted and chemical cell disruption methods, Can. J. Chem. Eng. 96 (2018) 1377–1381, https://doi.org/10.1002/cjce.23046.
[12] P.S. Saravana, V. Ummat, P. Bourke, B.K. Tiwari, Emerging green cell disruption techniques to obtain valuable compounds from macro and microalgae: a review, Crit. Rev. Biotechnol. (2022) 1–16, https://doi.org/10.1080/07388551.2022.2089869.
[13] B. Balasundaram, S. Harrison, D.G. Bracewell, Advances in product release strategies and impact on bioprocess design, Trends Biotechnol. 27 (2009) 477–485, https://doi.org/10.1016/j.tibtech.2009.04.004.
[14] T. Kotnik, L. Rems, M. Tarek, D. Miklavčič, Membrane Electroporation and Electropermeabilization: Mechanisms and Models, Annu. Rev. Biophys. 48 (2019) 63–91, https://doi.org/10.1146/annurev-biophys-052118-115451.
[15] D. Aguilar-Machado, C. Delso, J.M. Martinez, L. Morales-Oyervides, J. Montañez, J. Raso, Enzymatic Processes Triggered by PEF for Astaxanthin Extraction From Xanthophyllomyces dendrorhous, Front. Bioeng. Biotechnol. 8 (2020), https://doi.org/10.3389/fbioe.2020.00857.
[16] T. Raj, R. Morya, K. Chandrasekhar, D. Kumar, S. Soam, R. Kumar, A.K. Patel, S. H. Kim, Microalgae biomass deconstruction using green solvents: Challenges and future opportunities, Bioresour. Technol. 369 (2023), https://doi.org/10.1016/j.biortech.2022.128429.
[17] C.U. Mussagy, J.F.B. Pereira, V.C. Santos-Ebinuma, A. Pessoa, V. Raghavan, Insights into using green and unconventional technologies to recover natural astaxanthin from microbial biomass, Crit. Rev. Food Sci. Nutr. (2022), https://doi.org/10.1080/10408398.2022.2093326.
[18] J. Yu, X. Liu, L. Zhang, P. Shao, W. Wu, Z. Chen, J. Li, C.M.G.C. Renard, An overview of carotenoid extractions using green solvents assisted by Z-isomerization, Trends Food Sci. Technol. 123 (2022) 145–160, https://doi.org/10.1016/j.tifs.2022.03.009.
[19] J. Zuo, S. Geng, Y. Kong, P. Ma, Z. Fan, Y. Zhang, A. Dong, Current Progress in Natural Deep Eutectic Solvents for the Extraction of Active Components from Plants, Crit. Rev. Anal. Chem. 53 (2023) 177–198, https://doi.org/10.1080/10408347.2021.1946659.
[20] F.S.N. de Oliveira, A.R.C. Duarte, A look on target-specificity of eutectic systems based on natural bioactive compounds, in (2021) 271–307, https://doi.org/10.1016/bs.abr.2020.09.008.
[21] A. Mišan, M. Pojić, Applications of NADES in stabilizing food and protecting food compounds against oxidation, in (2021) 333–359, https://doi.org/10.1016/bs.abr.2020.09.010.
[22] A. Mišan, J. Nađpal, A. Stupar, M. Pojić, A. Mandić, R. Verpoorte, Y.H. Choi, The perspectives of natural deep eutectic solvents in agri-food sector, Crit. Rev. Food Sci. Nutr. 60 (2020) 2564–2592, https://doi.org/10.1080/10408398.2019.1650717.
[23] A.V. Chemat, K. Ravi, P. Hilali, Tixier, Review of Alternative Solvents for Green Extraction of Food and Natural Products: Panorama, Principles, Applications and Prospects, Molecules 24 (2019) 3007, https://doi.org/10.3390/molecules24163007.
[24] D.O. Abranches, J.A.P. Coutinho, Type V deep eutectic solvents: Design and applications, Curr Opin Green Sustain Chem. 35 (2022), 100612, https://doi.org/10.1016/j.cogsc.2022.100612.
[25] D.J.G.P. Van Osch, C.H.J.T. Dietz, S.E.E. Warrag, M.C. Kroon, The Curious Case of Hydrophobic Deep Eutectic Solvents: A Story on the Discovery, Design, and Applications, ACS Sustain. Chem. Eng. 8 (2020) 10591–10612, https://doi.org/10.1021/acssuschemeng.0c00559.
[26] C.U. Mussagy, V.C. Santos-Ebinuma, R.D. Herculano, J.A.P. Coutinho, J.F. B. Pereira, A. Pessoa, Ionic liquids or eutectic solvents? Identifying the best solvents for the extraction of astaxanthin and β-carotene from Phaffia rhodozyma yeast and preparation of biodegradable films, Green Chem. 24 (2022) 118–123, https://doi.org/10.1039/d1gc03521e.
[27] H. Zhang, B. Tang, K.H. Row, A Green Deep Eutectic Solvent-Based Ultrasound-Assisted Method to Extract Astaxanthin from Shrimp Byproducts, Anal. Lett. 47 (2014) 742–749, https://doi.org/10.1080/00032719.2013.855783.
[28] W. Pitacco, C. Samorì, L. Pezzolesi, V. Gori, A. Grillo, M. Tiecco, M. Vagnoni, P. Galletti, Extraction of astaxanthin from Haematococcus pluvialis with hydrophobic deep eutectic solvents based on oleic acid, Food Chem. 379 (2022), https://doi.org/10.1016/j.foodchem.2022.132156.
[29] J. Gao, J. You, J. Kang, F. Nie, H. Ji, S. Liu, Recovery of astaxanthin from shrimp (Penaeus vannamei) waste by ultrasonic-assisted extraction using ionic liquid-in-water microemulsions, Food Chem. 325 (2020), https://doi.org/10.1016/j.foodchem.2020.126850.
[30] Y.R. Lee, K.H. Row, Comparison of ionic liquids and deep eutectic solvents as additives for the ultrasonic extraction of astaxanthin from marine plants, J. Ind. Eng. Chem. 39 (2016) 87–92, https://doi.org/10.1016/j.jiec.2016.05.014.
[31] V. Chandra Roy, T.C. Ho, H.J. Lee, J.S. Park, S.Y. Nam, H. Lee, A.T. Getachew, B. S. Chun, Extraction of astaxanthin using ultrasound-assisted natural deep eutectic solvents from shrimp wastes and its application in bioactive films, J. Clean. Prod. 284 (2021), https://doi.org/10.1016/j.jclepro.2020.125417.
[32] C.A. Dos Santos, C.E.A. Padilha, K.S.F.S.C. Damasceno, P.I.P. Leite, A.C.J. De Araújo, P.R. Freitas, É.A. Vieira, A.M.T.M. Cordeiro, F.C. De Sousa, C.F. De Assis, Astaxanthin recovery from shrimp residue by solvent ethanol extraction using choline chloride: Glycerol deep eutectic solvent as adjuvant, J. Braz. Chem. Soc. 32 (2021) 1030–1039, https://doi.org/10.21577/0103-5053.20210005.
[33] P.I.P. Leite, C.F. de Assis, E. Silvino dos Santos, C.E. de A. Padilha, M. Ferrari, F. C. de Sousa Junior, Choline chloride-based deep eutectic solvents do not improve the ethanolic extraction of carotenoids from buriti fruit (Mauritia flexuosa L.), Sustain. Chem. Pharm. 20 (2021), https://doi.org/10.1016/j.scp.2021.100375.
[34] L.A. Rodrigues, C.V. Pereira, I.C. Leonardo, N. Fernández, F.B. Gaspar, J.M. Silva, R.L. Reis, A.R.C. Duarte, A. Paiva, A.A. Matias, Terpene-Based Natural Deep Eutectic Systems as Efficient Solvents to Recover Astaxanthin from Brown Crab Shell Residues, ACS Sustain. Chem. Eng. 8 (2020) 2246–2259, https://doi.org/10.1021/acssuschemeng.9b06283.
[35] F. Bergua, M. Castro, J. Muñoz-Embid, C. Lafuente, M. Artal, Hydrophobic eutectic solvents: Thermophysical study and application in removal of pharmaceutical products from water, Chem. Eng. J. 411 (2021), https://doi.org/10.1016/j.cej.2021.128472.
[36] F. Bergua, M. Castro, C. Lafuente, M. Artal, Thymol+l-menthol eutectic mixtures: Thermophysical properties and possible applications as decontaminants, J. Mol. Liq. 368 (2022), 120789, https://doi.org/10.1016/j.molliq.2022.120789.
[37] F. Bergua, M. Castro, J. Muñoz-Embid, C. Lafuente, M. Artal, L-menthol-based eutectic solvents: Characterization and application in the removal of drugs from water, J. Mol. Liq. 352 (2022), 118754, https://doi.org/10.1016/j.molliq.2022.118754.
[38] M.S. Blois, Antioxidant Determinations by the Use of a Stable Free Radical, Nature 181 (1958) 1199–1200, https://doi.org/10.1038/1811199a0.
[39] S.B. Kedare, R.P. Singh, Genesis and development of DPPH method of antioxidant assay, J. Food Sci. Technol. 48 (2011) 412–422, https://doi.org/10.1007/s13197-011-0251-1.
[40] E. Puértolas, E. Luengo, I. Álvarez, J. Raso, Improving Mass Transfer to Soften Tissues by Pulsed Electric Fields: Fundamentals and Applications, Annu. Rev. Food Sci. Technol. 3 (2012) 263–282, https://doi.org/10.1146/annurev-food-022811-101208.
[41] T.H.P. Brotosudarmo, L. Limantara, E. Setiyono, Heriyanto, Structures of Astaxanthin and Their Consequences for Therapeutic Application, Int, J. Food Sci. 2020 (2020) 1–16, https://doi.org/10.1155/2020/2156582.
[42] E.A.H.S.L. Luddecke, Use of carotenoidaggregates as colorants, USOO6827941B1, 2004.
[43] M.F. Nagoor Meeran, H. Javed, H. Al Taee, S. Azimullah, S.K. Ojha, Pharmacological properties and molecular mechanisms of thymol: Prospects for its therapeutic potential and pharmaceutical development, Front. Pharmacol. 8 (2017), https://doi.org/10.3389/fphar.2017.00380.
[44] C.J. Needs, P.M. Brooks, Clinical Pharmacokinetics of the Salicylates, Clin. Pharmacokinet. 10 (1985) 164–177, https://doi.org/10.2165/00003088-198510020-00004.
[45] A.D.D. Deutchoua, R. Siegnin, G.K. Kouteu, G.K. Dedzo, E. Ngameni, Electrochemistry of 2,2-Diphenyl-1-picrylhydrazyl (DPPH) in Acetonitrile in Presence of Ascorbic Acid - Application for Antioxidant Properties Evaluation, ChemistrySelect 4 (2019) 13746–13753, https://doi.org/10.1002/slct.201904082.
[46] M.C. Foti, Use and Abuse of the DPPH • Radical, J. Agric. Food Chem. 63 (2015) 8765–8776, https://doi.org/10.1021/acs.jafc.5b03839.
[47] K. Mishra, H. Ojha, N.K. Chaudhury, Estimation of antiradical properties of antioxidants using DPPH assay: A critical review and results, Food Chem. 130 (2012) 1036–1043, https://doi.org/10.1016/j.foodchem.2011.07.127.
[48] D. Beena, D.S. Kumar, Rawat, Synthesis and antioxidant activity of thymol and carvacrol based Schiff bases, Bioorg. Med. Chem. Lett. 23 (2013) 641–645, https://doi.org/10.1016/j.bmcl.2012.12.001.
[49] X. Zhang, X. Ren, X. Zhao, H. Liu, M. Wang, Y. Zhu, Stability, structure, and antioxidant activity of astaxanthin crystal from Haematococcus pluvialis, JAOCS, J. Am. Oil Chemists' Soc. 99 (2022) 367–377, https://doi.org/10.1002/aocs.12587.
[50] Y.M.A. Naguib, Antioxidant activities of astaxanthin and related carotenoids, J. Agric. Food Chem. 48 (2000) 1150–1154, https://doi.org/10.1021/jf991106k.
[51] T.N. Tran, N.-T. Tran, T.-A. Tran, D.-C. Pham, C.-H. Su, H.C. Nguyen, C.J. Barrow, D.-N. Ngo, Highly Active Astaxanthin Production from Waste Molasses by Mutated Rhodosporidium toruloides G17, Fermentation 9 (2023) 148, https://doi.org/10.3390/fermentation9020148.

[52] F. Abderrahim, S.M. Arribas, M.C. Gonzalez, L. Condezo-Hoyos, Rapid high-throughput assay to assess scavenging capacity index using DPPH, Food Chem. 141 (2013) 788–794, https://doi.org/10.1016/j.foodchem.2013.04.055.

[53] X. Li, D. Chen, G. Wang, Y. Lu, Investigation on the interaction between bovine serum albumin and 2,2-diphenyl-1-picrylhydrazyl, J. Lumin. 156 (2014) 255–261, https://doi.org/10.1016/j.jlumin.2014.08.025.

[54] O.P. Sharma, T.K. Bhat, DPPH antioxidant assay revisited, Food Chem. 113 (2009) 1202–1205, https://doi.org/10.1016/j.foodchem.2008.08.008.